Carbon Dioxide Radical Anion by Photoinduced Equilibration between Formate Salts and [^{11}C, ^{13}C, ^{14}C]CO_2 : Application to Carbon Isotope Radiolabeling

Augustin Malandain,[a] Maxime Molins,[a] Alexandre Hauwelle,[a, b] Alex Talbot,[a] Olivier Loreau,[a] Timothée D'Anfray,[a] Sébastien Goutal[b], Nicolas Tournier[b], Frédéric Taran,[a] Fabien Caillé,[b] Davide Audisio[a]*

[a] Université Paris-Saclay, CEA, Service de Chimie Bio-organique et Marquage, DMTS, F-91191, Gif-sur-Yvette, France. E-mail: davide.audisio@cea.fr

[b] Université Paris-Saclay, Inserm, CNRS, CEA, Laboratoire d'Imagerie Biomédicale Multimodale Paris-Saclay (BioMaps), F-91401 Orsay

Abstract:

The need for carbon-labeled radiotracers is increasingly higher in drug discovery and development (carbon-14, β^-, $t_{1/2}$ = 5730 years) as well as in PET, for *in vivo* molecular imaging applications (carbon-11, β^+, $t_{1/2}$ = 20.4 min). However, the structural diversity of radiotracers is still systematically driven by the narrow available labeled sources and methodologies. In this context, the emergence of carbon dioxide radical anion chemistry might set forth potential unexplored opportunities. Based on a dynamic isotopic equilibration between formate salts and [^{13}C, ^{14}C, ^{11}C]CO_2, C-labeled radical anion $CO_2^{\bullet-}$ could be accessed under extremely mild conditions within seconds. This methodology was successfully applied to hydro-carboxylation and bis-carboxylation reactions in late-stage carbon isotope labeling of pharmaceutically relevant compounds. The relevance of the method in applied radiochemistry was showcased by the whole-body PET biodistribution profile of [^{11}C]oxaprozin in mouse.

Introduction

The fixation of carbon dioxide (CO_2) and its valorization as a one-carbon (C1) building block has attracted considerable attention.[1] Carboxylation reactions have specifically benefited of extensive innovation and the use of CO_2 as an electrophilic partner, in transformations involving two-electron mechanisms, have been broadly explored.[2] Conversely, its single-electron reduction and the valorization of the corresponding radical anion ($CO_2^{\bullet-}$) in organic synthesis received less interest.[3] In 2017, seminal works by Jamison[4] reported a photoredox catalyzed access to $CO_2^{\bullet-}$ under ultraviolet irradiation (390 nm) and provided concrete evidence that single-electron reduction of CO_2 represents a productive strategy for C–C bond formation. A series of reports have shown improvement of the conditions, but the high reduction potential of CO_2 (E^0 = –2.21 V *vs* saturated calomel electrode (SCE) in DMF) renders this transformation challenging.[5] A significant step forward towards the mild formation of $CO_2^{\bullet-}$ was achieved from formate salts through a Hydrogen Atom Transfer (HAT).[6] This strategy was popularized in 2021 by the groups of Wickens and Li, who recognized that access to $CO_2^{\bullet-}$ was possible starting from formate salts, under photocatalytic conditions.[7,8] The radical anion was further engaged as nucleophilic carbon-radical in Giese type reactions.[9]

While advances in single-electron CO_2 chemistry provided a notable synthetic opportunity, this technology remains elusive for applications in the field of carbon-isotope radiolabeling. Carbon-11 (^{11}C, $t_{1/2}$ = 20.4 min, β^+ emitter) is a reference in positron emission tomography (PET) imaging; but it has a remarkably short half-life and can only be produced extemporaneously, on the nanomolar scale.[10] On the other hand, carbon-14 (^{14}C, $t_{1/2}$ = 5730 years, β^- emitter) is a pivotal tool for tracking the fate of organic compounds and a gold standard for human-ADME studies and crop science development, but the costs related to the source, its handling and the generation of long-lasting waste prevent the use of excess reagent.[11] Consequently, despite the fact that [^{14}C]CO_2 (1600 \$.mmol^{-1}) and [^{11}C]CO_2 are primary sources of both isotopes, such inherent challenges prevented using labeled $CO_2^{\bullet-}$ technologies.

At first sight, the HAT strategy from formate salts might appear promising, but unfortunately, limitations related to these radiolabeled C1 isotopologues precludes practical utilization. For instance, ^{14}C-formate, obtained from the reduction of CO_2 often in low chemical purity,[12] is commercially available in aqueous solutions at tenfold higher price than carbon dioxide ([^{14}C]HCOONa 16500 \$.mmol^{-1}). Notwithstanding the growing interest for the carbon dioxide radical anion, to the best of our knowledge, [^{11}C]$CO_2^{\bullet-}$ and [^{14}C]$CO_2^{\bullet-}$ remain elusive species, which have never been utilized in radiosynthesis, neither in PET nor in beta-imaging applications.

Herein, we report a strategy enabling access to labeled $CO_2^{\bullet-}$, based on the fast equilibration between [^{12}C]$CO_2^{\bullet-}$ and ^{11}C, ^{13}C and ^{14}C-labeled CO_2. Under mild photocatalytic conditions, formal reduction of [*C]CO_2 to H[*C]COO^- takes place within seconds and the generated [*C]$CO_2^{\bullet-}$ was reacted in Giese-type radical transformations to access to pharmaceutically relevant labeled derivatives. In the process, we discovered an unexpected amide bond rearrangement and accessed to labeled succinimide isotopomers. The relevance of this technology was highlighted by the synthesis of radiotracers with both long- and short-lived carbon isotopes and with the productive ^{14}C-^{12}C and ^{11}C-^{12}C bond formation to access [^{14}C]mesuximide and [^{11}C]oxaprozine. As a proof-of-concept of *in vivo* feasibility, the biodistribution of [^{11}C]oxaprozin was realized by *in vivo* PET imaging in mice.

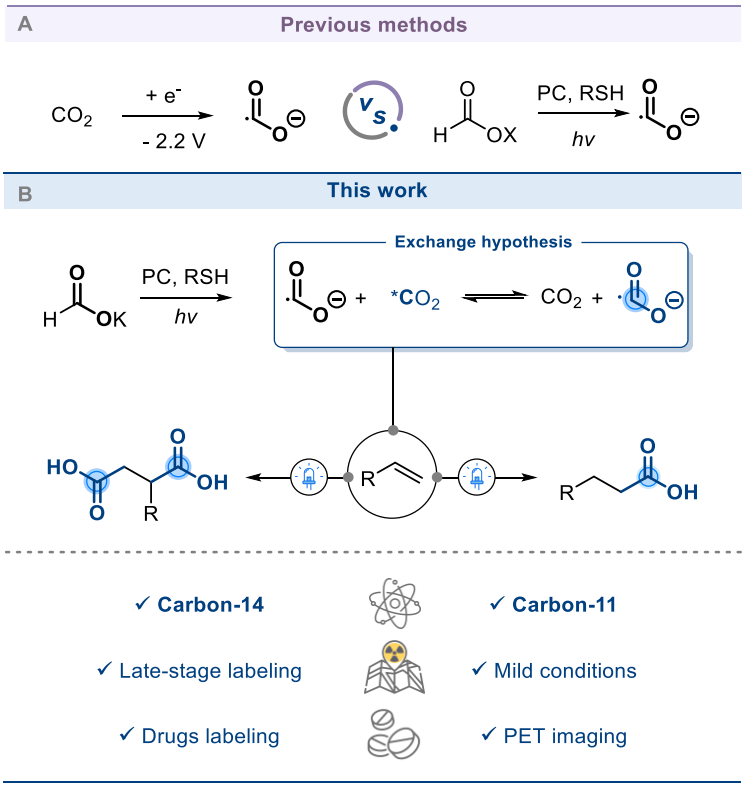

Scheme 1. A) Current state-of-the-art to access to carbon dioxide radical anion. B) Working hypothesis on the equilibration between [^{12}C]carbon dioxide radical anion and C-labeled CO_2; opportunities for late-stage ^{14}C and ^{11}C labeling. PC : photocatalyst.

Results and discussion

To enable simple access to C-labeled $CO_2^{\bullet-}$ directly from *C-labeled CO_2, it was hypothesized that *in situ* generation of [^{12}C]$CO_2^{\bullet-}$ from ^{12}C-formate might trigger a reversible redox process in presence of C-labeled CO_2, to form the desired [$^{11/14}$C]$CO_2^{\bullet-}$. While appealing, a number of challenges and pitfalls were anticipated. For instance, the rate of equilibration that has to match with the short half-life of ^{11}C and the inherent stability of the radical anion species, which might undergo accelerated radiolysis (*i.e.* decomposition due to ionizing radiation) related to the decay energy of the radioisotopes. With such questions in mind, we commenced our investigations looking for proof-of-concept to validate the hypothesis using stable labeled [^{13}C]CO_2. When a dimethyl sulfoxide (DMSO) solution of potassium formate [^{12}C]HCOOK in presence of organic photocatalyst 4CzIPN (5 mol%) and 1.5 equiv. of [^{13}C]CO_2 was irradiated under blue light (460 nm), the formation of [^{13}C]HCOOK was observed (Scheme 2A). The

isotopic enrichment (IE) was shown by the appearance of two satellites at δ = 8.58 and 8.13 ppm in the ^{1}H-NMR and the signal of ^{13}C-labeled formate in the ^{13}C-NMR at δ = 167 ppm (see supporting information). Thought the observed IE of 42% was moderate, the overall process is equivalent to the formal reduction of [^{13}C]CO_2 to [^{13}C]HCOOK, a transformation which usually requires the provision of an important source of energy[13] or highly reductant photocatalysts.[14]

After optimization (Scheme 2A), the use of 4DPAIPN (5 mol%) and thiol T1 (10 mol%) in DMSO-d_6 allowed to form [^{13}C]HCOOK in 50% IE after 2 hours, nearly the maximal theoretical value under such stoichiometry.[15] 4DPAIPN could be replaced by 4CzIPN without any significant drop in the final IE.

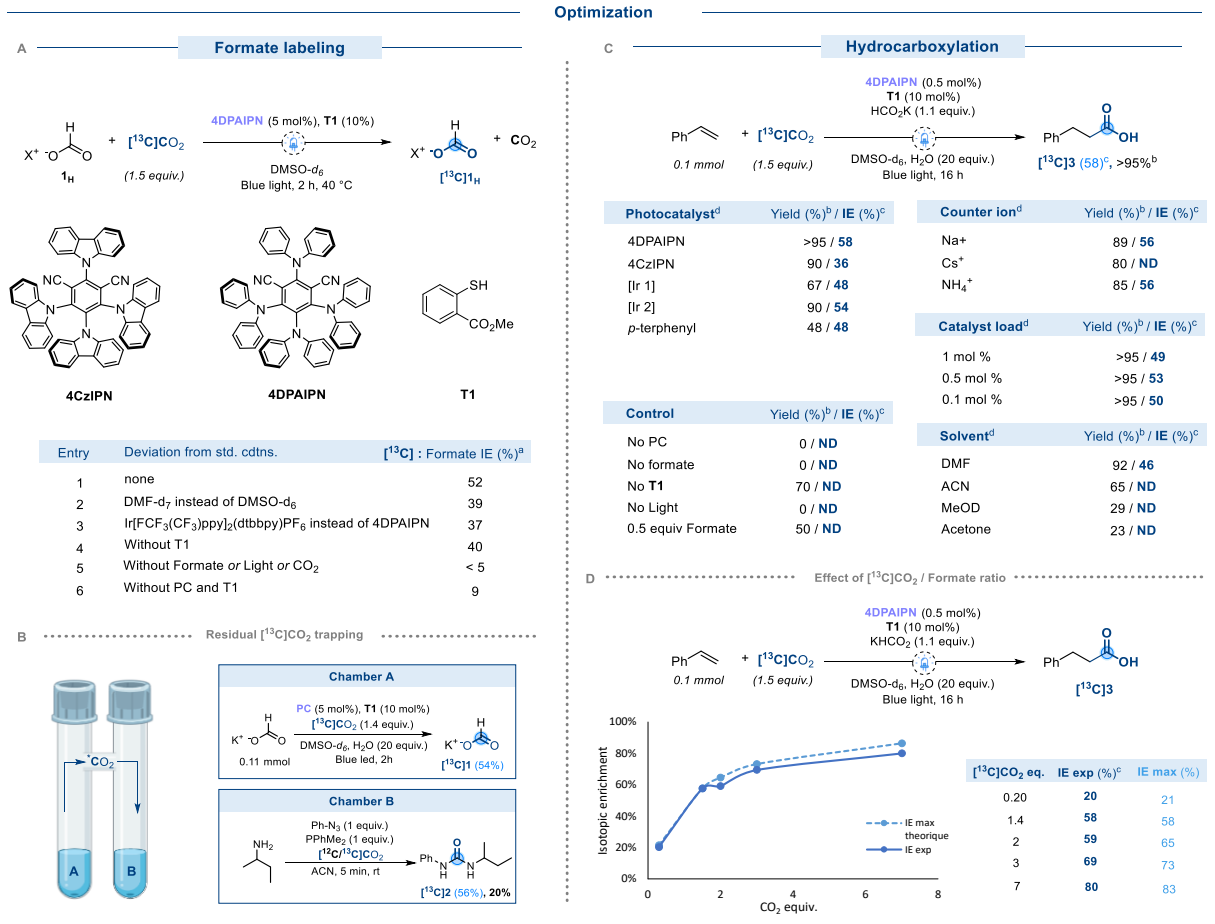

Scheme 2. Optimization of formate labeling with [^{13}C]CO_2 and its application to hydro-carboxylation.[a] Isotopic enrichment determined by ^{1}H NMR. [b] Yields determined by ^{1}H NMR using dibromomethane as internal standard. [c] Isotopic enrichment determined by MS. ND: not determined. [d] reactions performed using 5 mol% of photocatalyst.

The photoinduced equilibration was next performed in a two-chamber reactor (Ch.A), and in the adjacent chamber (Ch.B) a Staudinger/aza-Wittig sequence[16] was set to react with the residual [^{13}C]CO_2 (Scheme 2B). Pleasingly, urea **[^{13}C]2** was isolated in 56% IE, thus confirming that a nearly identical isotopic dilution occurred in the headspace.

To confirm the formation of the transient [^{13}C]$CO_2^{\bullet-}$, we explored the reaction in presence of styrene. In the optimized conditions, the presence of H_2O (20 equiv.) was essential for cleaner crude reaction and **[^{13}C]3** was obtained in >95% NMR yield and 58% IE (Scheme 2C). The effect of the stoichiometry of [^{13}C]CO_2 was next studied and the addition of precise equivalents of [^{13}C]CO_2 was performed using a RC Tritec carboxylation manifold. Pleasingly, the experimental IE nearly overlapped with the expected theoretical values (Scheme 2D). This is a crucial factor for applications to ^{14}C-radiolabeling, where the control of molar activity (A_m) is a strict requirement for *in vitro* and *in vivo* studies.

With this optimized procedure, we set out to investigate the scope of the transformation on a series of olefin derivatives (Scheme 3). Styrenes could be hydro-carboxylated with yields spanning from 34% to 93% and IE close to the theoretical maxima. A good tolerance was observed with diverse *para*- and *meta*-substituents (Scheme 3A). Cyclic dihydronaphthalene **[^{13}C]3j** was converted with moderate yield and 58% IE. The conditions were applicable to substrates bearing functional groups such as primary amines **[^{13}C]3g**, boronic acid **[^{13}C]3f** and aryl chloride **[^{13}C]3e**. The presence of bromine substituents, whether on the aromatic part or the alkene, lead to significant loss of yield.[17] The presence of methyl was well tolerated on *α* position **[^{13}C]3a**. Contrariwise, *β*-substituted styrenes did not react (see SI). On the other hand, 1,1-diphenylethylene derivatives **[^{13}C]3k-3m** were carboxylated in 67 to 96% yields and optimal IE.

N-monosubstituted acrylamides reacted smoothly to provide the corresponding 4-amino-4-oxobutanoic acids **[^{13}C]4a-4f** in moderate to good yields and IE (Scheme 3B). Acrylate and acrylonitrile provided **[^{13}C]4g** and **[^{13}C]4h** in 30 and 78% yield with 31 and 20% IE, respectively. Interestingly, substitutions on the acrylate were tolerated with no impact on either yields or IEs

[^{13}C]4b-4d. Dehydroalanine (Dha) is an amino acid, found primarily in peptides.[18] This non-proteinogenic residue provides strong chemical utility in proteins and was pioneered by the Davis group and others.[19] Under standard conditions, protected Dha was converted into aspartic acid **[^{13}C]4f** in 33% yield and 50% IE, offering a complementary strategy to access to this labeled amino acid.[20]

Intriguingly, when *N,N*-disubstituted acrylamides were subjected to identical reaction conditions, we observed systematically two labeled signals in the ^{13}C-NMR spectra **[^{13}C]6a-6h**. To disentangle such unexpected results, we focused on product **[^{13}C]6a**. As shown in Scheme 3D, mass spectrometry indicated incorporation of only one ^{13}C in the product with 50% IE, excluding doubly labeled product. Comparing with the unlabeled [**^{12}C**]**6a**, prepared by reacting succinic anhydride with corresponding piperidine, we confirmed that the ^{13}C-signal at 170.2 ppm belonged to the carbonyl of the amide (C_4). Additional evidence was provided by the appearance of resonance doublets corresponding to the methylene groups C_2 and C_3 in *alpha* to the carboxylic acid (C_1) and amide (C_4), of the 4-amino-4-oxobutanoic acid, with C_1-C_2 (d, δ = 29.8 ppm, $J_{C1\text{-}C2}$ = 56 Hz) and C_4-C_3 (d, δ = 28.2 ppm, $J_{C4\text{-}C3}$ = 51 Hz) coupling constants. While initial ^{13}C-NMR spectra (D1 = 4 sec) seemed to point to a higher ^{13}C enrichment of C_1, quantitative analysis (D1 = 20 sec) showed equal enrichment. MS/MS fragmentations confirmed this ratio and determined that C_1 and C_4 are both enriched at 25% IE. These results confirmed that **[^{13}C]6a** was obtained as mixture of two inseparable isotopomers. Additional investigation highlighted that the rearrangement is complete within 10 minutes and no further isotope incorporation took place when **[^{12}C]6a** was reengaged under standard reaction conditions (see SI for details). Since formation of isotopomers was observed exclusively in presence of *N,N*-disubstituted acrylamides, this unexpected behavior might be related to the steric hindrance at the nitrogen (NR_2), which decreases the barrier for N-CO rotation and twist more freely than secondary amides, as previously reported by Lloyd-Jones and Booker-Milburn.[21]

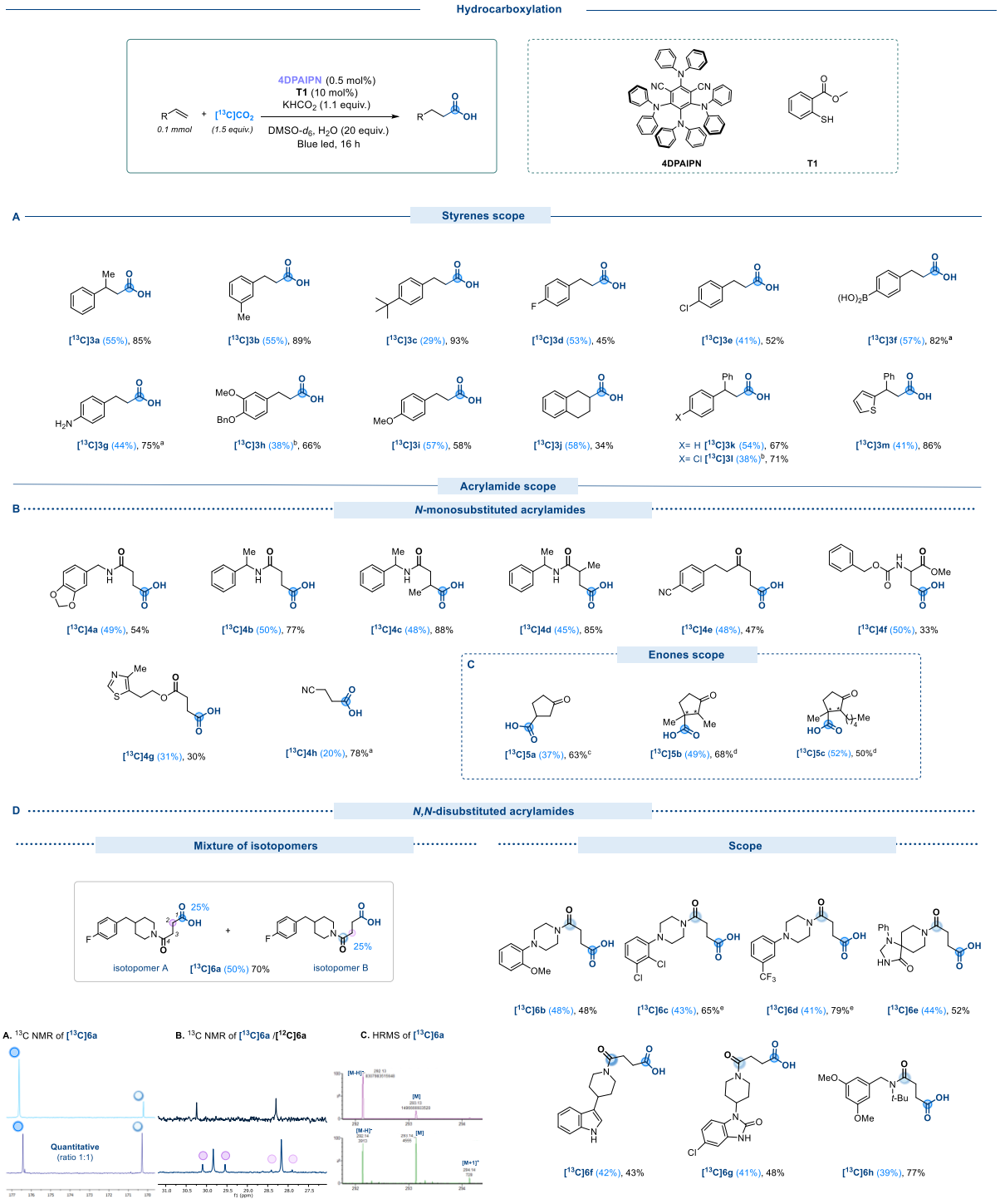

Scheme 3: Investigation of the scope of the hydrocarboxylation reaction. Isolated yields unless otherwise stated. IE are shown in blue under brackets. [a] Yields determined by ^{1}H NMR using dibromomethane as internal standard. [b] Reaction performed on 0.5 mmol scale using 0.5 equiv. of $[^{13}C]CO_2$. [c] Isolated as hydrazone. [d] Isolated as a mixture of diastereoisomers. [e] Reaction time: 1 hour.

We speculate that after radical carboxylation with [^{13}C]$CO_2^{\bullet-}$, the carbon-radical in *alpha* to the amide (trapped in presence of TEMPO, see SI for details) is next converted into an anionic adduct *via* a reductive radical/polar crossover process thought single electron transfer (SET).[22] This carboxylate intermediate might undergo cyclisation to generate the transient mono-labeled succinic anhydride and the piperidine anion. Further nucleophilic addition onto the anhydride provides a mixture of isotopomers (see SI for details). While so far attempts to trap the labeled succinic anhydride with additional nucleophiles have been unsuccessful, the overall outcome of this transformation allows inserting a carbon isotope into a substituted alkyl amide in one single step from CO_2. Scaffolds of interest were well tolerated including 1,3,8-triazaspiro[4.5]decan-4-one **[^{13}C]6e**,[23] and in the same vein, sensitive acrylamides were easily converted into potent drug precursors with good yields and IE **[^{13}C]6c**.[24]

Pleasingly, pharmaceutical derivatives such as FDA approved doxepine and ibrutinib were functionalized to the corresponding acids **[^{13}C]7a-7b** in 18% and 33% yield and suitable IE (Scheme 4A). In addition, 4,5-diphenyl-2-vinyloxazole reacted in presence of [^{13}C]CO_2 to provide oxaprozine **[^{13}C]7c**, a commercial nonsteroidal anti-inflammatory drug, in one-single step.[25] Previously, [^{14}C]oxaprozin was labeled from [1,4-^{14}C]succinic anhydride in presence of benzoin.[26] Labeled succinic anhydride is an elaborated precursor obtained in four steps from [^{14}C]CO_2, by sequential cyanation of dibromoethane, nitrile hydrolysis and succinic acid dehydration.[27] The direct labeling of **[^{13}C]7c** exemplifies how radiochemistry can benefit from this late-stage approach.

Furthermore, in presence of 3 equiv. of [^{13}C]CO_2, **S22** provided labeled *N*-acetyl phenylalanine **[^{13}C]7d** in 57% yield and 20% IE.[28] While this result opens a new avenue to labeled phenylalanine derivatives, according to the reported reduction potential, **S22** (E_{red} = - 1.60 to - 1.70 V *vs.* SCE)[29] should undergo SET olefin reduction in presence of $CO_2^{\bullet-}$, rather than hydro-carboxylation, as previously shown by Jui.[30] Indeed, under identical conditions, the corresponding methyl ester underwent selective olefin reduction. However, our results indicate that a different reaction pathway takes place under our reaction conditions, favoring hydro-

carboxylation of **S22**, leading to the formation of a malonate intermediate, which undergoes Krapcho decarboxylation to provide **[^{13}C]7d**.[31]

Alkene bis-carboxylation was next investigated, as alternative to label succinimides (Scheme 4B).[32] To promote the bis-carboxylation, an optimization of the reaction condition was performed with only 2 equiv. of labeled CO_2 (see SI for details). In presence of DABCO (10 mol%) and molecular sieves (4 Å), the corresponding succinic acids **[^{13}C]8a-8f** were isolated with both carbonyl positions labeled in 33% to 43% single and 31% to 48% double ^{13}C incorporation (Scheme 4B). Subsequent cyclisation in presence of trifluoroacetic anhydride (TFAA)[33] and reaction with primary amines in refluxing acetic acid[34] delivered the desired double-labeled succinimides without loss of isotope incorporation. In the event, mesuximide **[^{13}C]9f**, an anticonvulsant sold as a racemate, was isolated 33% yield and 39% single and 46% double enrichment. The peculiar isotopic pattern was confirmed by ^{13}C-NMR spectra, showing resonance doublets corresponding (d, δ = 181.2 ppm, $J_{C1\text{-}C2}$ = 13.5 Hz, Scheme 4E).

To showcase the modularity of the approach, cyclization of 4-amino-4-oxobutanoic acids **[^{13}C]4b**, **[^{13}C]4c** and **[^{13}C]4d** in presence of $ZnCl_2$ and hexamethyldisilazane (HMDS) enabled the formation of single-labeled succinimides **[^{13}C]9g-9i** (Scheme 4D).

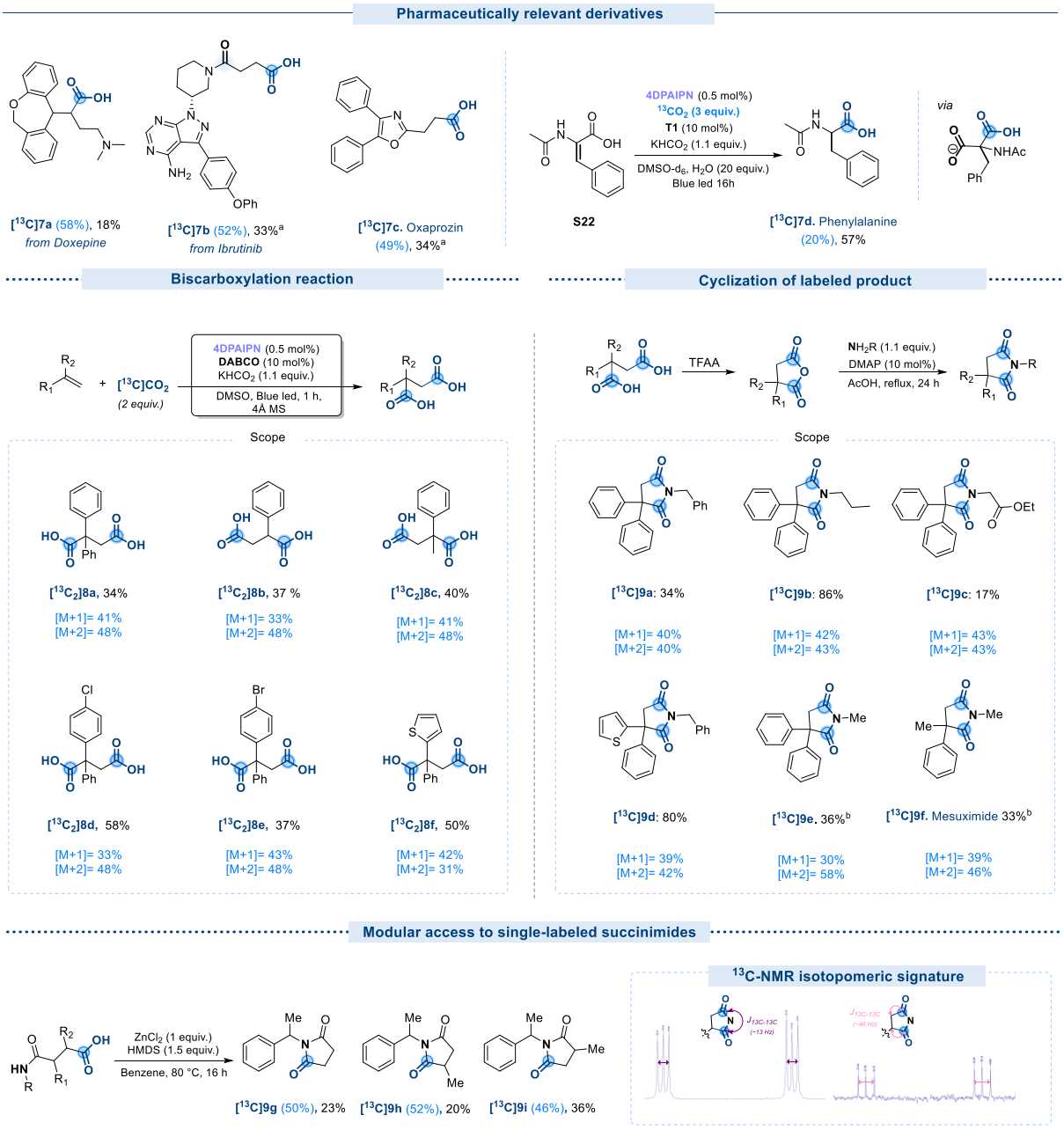

Scheme 4: A) Labeling of pharmaceutically relevant derivatives. B) Scope of the bis-carboxylation. C, D and E) Application to the preparation of labeled succinimides. [a] Reaction time 1 hour. [b] $MeNH_2.HCl$ (5 equiv.).

While the photoinduced equilibration has shown potential for isotope labeling, questions remained about its applications to radiocarbons, as no data is available on the stability of $CO_2^{\bullet-}$ in presence of β^+ or β^- emission. When the hydro-carboxylation of styrene was performed with radioactive $[^{14}C]CO_2$ (1.5 equiv.), pleasingly, a clean reaction was observed and after radio-

HPLC purification **[^{14}C]4d** (Scheme 5) was isolated in 56% yield and 53% IE, corresponding to a molar activity (A_m) of 1.22 GBq.mmol^{-1}. To the best of our knowledge, this is the first time [^{14}C]$CO_2^{\bullet-}$ was generated and utilized for productive ^{12}C-^{14}C bond formation. Furthermore, **[^{14}C]4d** could potentially be valorized in the synthesis of prodrugs such as Gemcitabine.[35] Next, the bis-carboxylation allowed to obtain **[^{14}C]8c**, which was engaged in the cyclization/substitution procedure to access to ^{14}C-double-labeled mesuximide **[^{14}C]9f** in high A_m. These strategies provide an advantageous and complementary alternative to the state-of-the art and offer a late-stage access to radiopharmaceuticals for ADME studies.

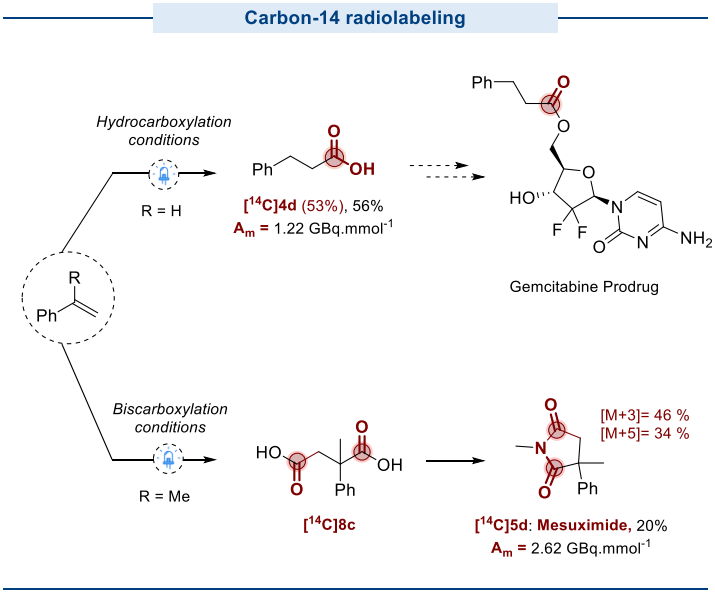

Scheme 5: Labeling of pharmaceutically relevant substrates with ^{14}C. See SI for experimental details.

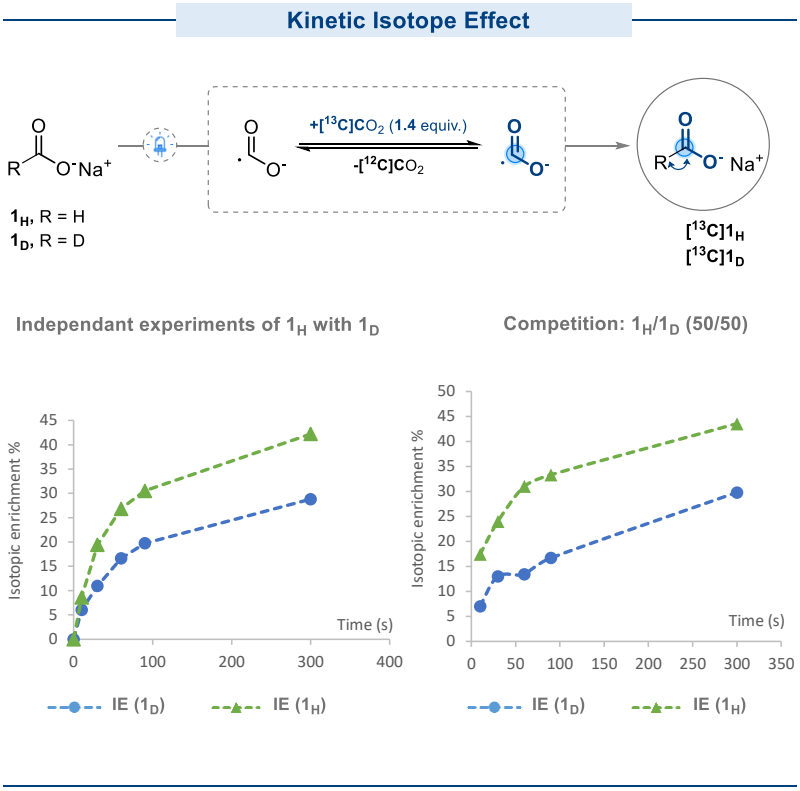

Scheme 6: Kinetic investigations from **[^{12}C]1$_H$** and **[^{12}C]1$_D$**. See SI for experimental details.

To evaluate the compatibility with the short half-life of ^{11}C, kinetic experiments on the isotopic equilibration were performed (Scheme 6). Pleasingly, formation of **[^{13}C]1$_H$** was observed within seconds from **[^{12}C]1$_H$**, after irradiation. When the reaction was separately repeated starting from **[^{12}C]1$_D$** and 20 equiv. of D_2O, a lower rate of ^{13}C incorporation was observed with a KIE of 1.8. In addition, competitive experiments starting from a 1/1 mixture of **[^{12}C]1$_H$** and **[^{12}C]1$_D$** in presence of H_2O (10 equiv.) / D_2O (10 equiv.) showed that % IE of **[^{13}C]1$_H$** over **[^{13}C]1$_D$** was systematically higher in favor of the proton-containing isotopologue. These results seem to indicate the cleavage of the C-H bond of formate as the rate-limiting step of the process.[36]

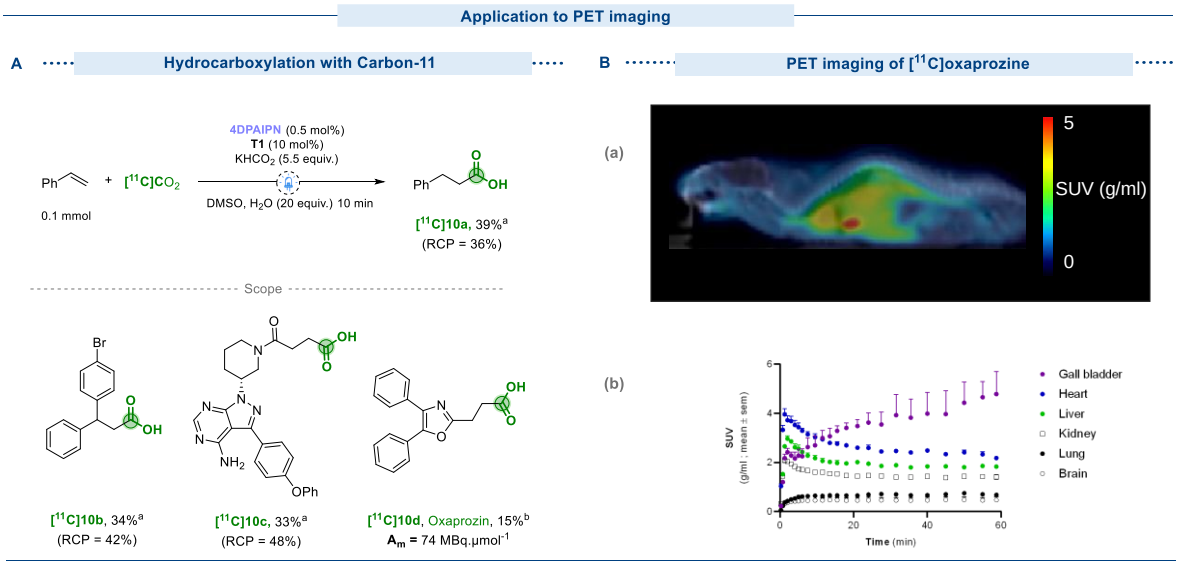

Scheme 7: A) ^{11}C-labeling. [a] Radiochemical conversion = (A_{EOS} / A_{CO2}) x RCP with A_{EOS} = decay-corrected activity at the end of the synthesis and A_{CO2} = starting activity of [^{11}C]CO_2. [b] Radiochemical yield. B) Biodistribution of [^{11}C]10d in the mouse whole body. (a) Average microPET images of [^{11}C]10d in mice using standard uptake values (SUV) over 60-min acquisition. Parametric microPET images are overlaid onto a CT mouse for anatomical localization. (b) Time-activity curves of regional [^{11}C]10d, expressed as SUV values *vs* time.

The fast isotope equilibration opened a window of opportunity for ^{11}C-radiolabeling. When the standard reaction conditions were applied with [^{11}C]CO_2, a 8% radiochemical conversion (RCC) was observed. After optimization, excess of formate (5.5 equiv. in respect to styrene) under 10 min blue LED irradiation allowed to obtain **[^{11}C]10a** in 39% RCC. With these conditions in hand, **[^{11}C]10b** and **[^{11}C]10c** were labeled in 34 and 33% RCC, respectively. To go further, automated radiosynthesis of [^{11}C]oxaprozin **[^{11}C]10d** afforded the ready-to-inject radiotracer in 15% RCY and 74 MBq.µmol^{-1} A_m. It is important to highlight that **[^{11}C]10d** has previously been labeled by Szikra *et al*. in a two-step sequence from a Grignard precursor.[37]

To show concrete evidence of the utility of the approach for *in vivo* imaging, the whole-body PET biodistribution profile of [^{11}C]oxaprozin was investigated in mice (Scheme 7*a*). The time-activity curves (TACs) depict a rapid uptake of **[^{11}C]10d** in heart, liver and kidney followed by

a slow distribution phase (scheme 7B). High level of radioactivity in the gallbladder is consistent with the previously reported biliary elimination of oxaprozin and/or its metabolites.[23] No radioactivity could be found in the urinary bladder, which suggests limited importance of the urinary pathway for the elimination of [^{11}C]oxaprozin or its radiometabolite(s) in mice. The distribution of **[^{11}C]10d** in the brain and peripheral tissues is consistent with the low volume of distribution of oxaprozin estimated in humans, which indicates limited extravascular distribution.[23]

Conclusion

In conclusion, we have developed a photocatalytic synthetic access to $CO_2^{\bullet-}$ from isotopically labeled CO_2 and [^{12}C]formate salts. This strategy allows the formal reduction of ^{11,} ^{13,} ^{14}C labeled CO_2 to HCOOK under mild conditions and was applied to the Giese-type hydrocarboxylation to label effectively carboxylic acids, including pharmaceutical derivatives. When applied to *N,N*-disubstituted acrylamides a rearrangement of the succinic acid moiety was observed. This unexpected result allowed to obtain the corresponding label tertiary amides in one-step from CO_2. When the equilibration process was implemented towards the bis-carboxylation of styrenes, doubly-labeled derivatives could be reached efficiently. The modularity of the approach was especially useful towards the labeling of succinimides. The current study demonstrated the possibility to generate and use [^{11}C] and [^{14}C]$CO_2^{\bullet-}$ in radical addition reactions. The convenience of this novel late-stage radio-carboxylation tool was demonstrated by accessing [^{11}C]oxaprozin ready-to-inject radiotracer for PET imaging applications.

Acknowledgements

This work was supported by CEA and the European Union's Horizon 2020 research and innovation program under the European Research Council (ERC-2019-COG – 864576). The

authors thank A. Goudet, S. Lebrequier and D.-A. Buisson (DRF-JOLIOT-SCBM, CEA) for the excellent analytical support.

Competing interests

The authors declare no competing interests

Keywords: Carbon-14 • Carbon-11 • Carbon Dioxide Radical Anion• PET imaging • Isotope Labeling

References

(1) a) Aresta, M.; Dibenedetto, A.; Angelini, A., Catalysis for the Valorization of Exhaust Carbon: from CO_2 to Chemicals, Materials, and Fuels. Technological Use of CO_2. *Chem. Rev.* **2014**, *114*, 1709-1742. b) M. Aresta, Carbon dioxide as chemical feedstock, Wiley, Hoboken, **2010**.
(2) a) Dabral, S. & Schaub, T. The Use of Carbon Dioxide (CO_2) as a Building Block in Organic Synthesis from an Industrial Perspective. *Adv. Syn. Catal.* **2019**, *361*, 223–246. b) Tortajada, A.; Juliá-Hernández, F.; Börjesson, M.; Moragas, T.; Martin, R., Transition-Metal-Catalyzed Carboxylation Reactions with Carbon Dioxide. *Angew. Chem., Int. Ed.* **2018**, *57*, 15948-15982. c) Liu, Q., Wu, L., Jackstell, R. & Beller, M. Using carbon dioxide as a building block in organic synthesis. *Nat. Commun.* **2015**, *6*, 5933. d) Cauwenbergh, R.; Goyal, V.; Maiti, R.; Natte, K.; Das, S., Challenges and recent advancements in the transformation of CO_2 into carboxylic acids: straightforward assembly with homogeneous 3d metals. *Chem. Soc. Rev.* **2022**, *51*, 9371-9423. e) Yang, Y.; Lee, J.-W., Toward ideal carbon dioxide functionalization. *Chem. Sci.* **2019**, *10*, 3905-3926.
(3) a) Morgenstern, D. A.; Wittrig, R. E.; Fanwick, P. E.; Kubiak, C. P. Photoreduction of carbon dioxide to its radical anion by nickel cluster $[Ni_3(\mu_3\text{-}I)_2(dppm)_3]$: formation of two carbon-carbon bonds via addition of carbon dioxide radical anion to cyclohexene. *J. Am. Chem. Soc.* **1993**, *115*, 6470-6471. b) Otero, M. D.; Batanero, B.; Barba, F. CO_2 anion–radical in organic carboxylations.*Tetrahedron Lett.* **2006**, *47*, 2171-2173. c) Mello, R.; Arango-Daza, J. C.; Varea, T.; González-Núñez, M. E. Photoiodocarboxylation of Activated C═C Double Bonds with CO_2 and Lithium Iodide. *J. Org. Chem.* **2018**, *83*, 13381–13394.
(4) a) Seo, H.; Katcher, M. H.; Jamison T. F. Photoredox activation of carbon dioxide for amino acid synthesis in continuous flow *Nat. Chem.* **2017**, *9*, 453-456. b) Seo, H.; Liu, A.; Jamison, T. F. Direct β-Selective Hydrocarboxylation of Styrenes with CO_2 Enabled by Continuous Flow Photoredox Catalysis. *J. Am. Chem. Soc.* **2017**, *139*, 13969-13972.
(5) a) Ye, J.-H.; Miao, M.; Huang, H.; Yan, S.-S.; Yin, Z.-B.; Zhou, W.-J.; Yu, D.-G. Visible-Light-Driven Iron-Promoted Thiocarboxylation of Styrenes and Acrylates with CO_2. *Angew. Chem., Int. Ed.* **2017**, *56*, 15416-15420. b) Huang, H.; Ye, J.-H.; Zhu, L.; Ran, C.-K.; Miao, M.; Wang, W.; Chen, H.; Zhou, W.-J.; Lan, Y.; Yu, B.; Yu, D.-G. Visible-Light-Driven Anti-Markovnikov Hydrocarboxylation of Acrylates and Styrenes with CO_2. *CCS Chem.* **2021**, *3*, 1746-1756. c) Ju, T.; Zhou, Y.-Q.; Cao, K.-G.; Fu, Q.; Ye, J.-H.; Sun, G.-Q.; Liu, X.-F.; Chen, L.; Liao, L.-L.; Yu, D.-G., Dicarboxylation of alkenes, allenes and (hetero)arenes with CO_2 via visible-light photoredox catalysis. *Nat. Catal.* **2021**, *4*, 304-311. d) Song, L.; Wang, W.; Yue, J.-P.; Jiang, Y.-X.; Wei, M.-K.; Zhang, H.-P.; Yan, S.-S.; Liao, L.-L.; Yu, D.-G. Visible-light photocatalytic di- and hydro-carboxylation of unactivated alkenes with CO_2. *Nat. Catal.* **2022**, *5*, 832-838.
(6) Selected reviews for HAT: a) Cao, H.; Tang, X.; Tang, H.; Yuan, Y.; Wu, J. *Chem Catal.* **2021**, *1*, 523–598. b) Capaldo, L.; Ravelli, D.; Fagnoni, M. *Chem. Rev.* **2022**, *122*, 1875–1924.
(7) Alektiar, S. N.; Wickens, Z. K. Photoinduced Hydrocarboxylation via Thiol-Catalyzed Delivery of Formate Across Activated Alkenes. *J. Am. Chem. Soc.* **2021**, *143*, 13022–13028.

(8) Huang, Y.; Hou, J.; Zhan, L.-W.; Zhang, Q.; Tang, W.-Y.; Li, B.-D., Photoredox Activation of Formate Salts: Hydrocarboxylation of Alkenes via Carboxyl Group Transfer. *ACS Catal.* **2021**, *11*, 15004-15012.
(9) a) Wang, H.; Gao, Y.; Zhou, C.; Li, G. Visible-Light-Driven Reductive Carboarylation of Styrenes with CO_2 and Aryl Halides. *J. Am. Chem. Soc.* **2020**, *142*, 8122-8129. b) Chmiel, A. F.; Williams, O. P.; Chernowsky, C. P.; Yeung, C. S.; Wickens, Z. K. Non-innocent Radical Ion Intermediates in Photoredox Catalysis: Parallel Reduction Modes Enable Coupling of Diverse Aryl Chlorides. *J. Am. Chem. Soc.* **2021**, *143*, 10882-10889. c) Campbell, M. W.; Polites, V. C.; Patel, S.; Lipson, J. E.; Majhi, J.; Molander, G. A. Photochemical C–F Activation Enables Defluorinative Alkylation of Trifluoroacetates and -Acetamides. *J. Am. Chem. Soc.* **2021**, *143*, 19648–19654. d) Xu, P.; Wang, S.; Xu, H.; Liu, Y.-Q.; Li, R.-B.; Liu, W.-W.; Wang, X.-Y.; Zou, M.-L.; Zhou, Y.; Guo, D.; Zhu, X. Dicarboxylation of Alkenes with CO_2 and Formate via Photoredox Catalysis. *ACS Catal.* **2023**, *13*, 2149-2155. e) Fu, M.-C.; Wang, J.-X.; Ge, W.; Du, F.-M.; Fu, Y. Dual nickel/photoredox catalyzed carboxylation of C(sp^2)-halides with formate. *Org. Chem. Front.* **2023**, *10*, 35-41. f) Mangaonkar, S. R.; Hayashi, H.; Takano, H.; Kanna, W.; Maeda, S.; Mita, T. Photoredox/HAT-Catalyzed Dearomative Nucleophilic Addition of the CO_2 Radical Anion to (Hetero)Aromatics. *ACS Catal.* **2023**, *13*, 2482-2488.
(10) a) Deng, X.; Rong, J.; Wang, L.; Vasdev, N.; Zhang, L.; Josephson, L.; Liang, S. H. Chemistry for Positron Emission Tomography: Recent Advances in ^{11}C-, ^{18}F-, ^{13}N-, and ^{15}O-Labeling Reactions. *Angew. Chem., Int. Ed.* **2019**, *58*, 2580–2605. b) Rotstein, B. H.; Liang, S. H.; Placzek, M. S.; Hooker, J. M.; Gee, A. D.; Dollé, F.; Wilson, A. A.; Vasdev, N. ^{11}C═O bonds made easily for positron emission tomography radiopharmaceuticals. *Chem. Soc. Rev.* **2016**, *45*, 4708–4726. c) Taddei, C.; Pike, V. W. [^{11}C]Carbon monoxide: advances in production and application to PET radiotracer development over the past 15 years. *EJNMMI Radiopharmacy and Chemistry* **2019**, *4*.
(11) a) Babin, V.; Taran, F.; Audisio, D. Late-Stage Carbon-14 Labeling and Isotope Exchange: Emerging Opportunities and Future Challenges. *JACS Au* **2022**, *2*, 1234–1251. b) Elmore, C. S.; Bragg, R. A. Isotope chemistry; a useful tool in the drug discovery arsenal. *Bioorg. Med. Chem. Lett.* **2015**, *25*, 167–171. c) Isin, E. M.; Elmore, C. S.; Nilsson, G. N.; Thompson, R. A.; Weidolf, L. Use of Radiolabeled Compounds in Drug Metabolism and Pharmacokinetic Studies. *Chem. Res. Toxicol.* **2012**, *25*, 532–542.
(12) Mixture of by-products residual from the prior reduction step are often present this ^{14}C-labeled reagent. See: Whitehead, D. M.; Hartmann, S.; Ilyas, T.; Taylor, K. R.; Kohler, A. D.; Ellames, G. J. A convenient method to produce [^{14}C]carbon monoxide and its application to the radiosynthesis of [*carboxyl*-^{14}C]celivarone, [*carboxyl*-^{14}C]SSR149744. *J. Label. Compd. Radiopharm.* **2013**, *56*, 36–41.
(13) You, Y.; Kanna, W.; Takano, H.; Hayashi, H.; Maeda, S.; Mita, T. Electrochemical Dearomative Dicarboxylation of Heterocycles with Highly Negative Reduction Potentials. *J. Am. Chem. Soc.* **2022**, 144, 3685–3695.
(14) Matsuoka, S.; Kohzuki, T.; Pac, C.; Ishida, A.; Takamuku, S.; Kusaba, M.; Nakashima, N.; Yanagida, S. Photocatalysis of oligo(*p*-phenylenes): photochemical reduction of carbon dioxide with triethylamine. *J. Phys. Chem.* **1992**, 96, 11, 4437–4442
(15) Under these stoichiometry, the maximum theoretical IE is 1.4 equiv. *$^{13}CO_2$/(1.4 equiv. *$^{13}CO_2$ + 1 equiv. $^{12}CO_2$ substrate)x100 = 58%. For example, see: Talbot, A.; Sallustrau, A.; Goudet, A.; Taran, F.; Audisio, D. Investigation on the Stoichiometry of Carbon Dioxide in Isotope-Exchange Reactions with Phenylacetic Acids. *Synlett* **2022**, *33*, 171–176.
(16) Del Vecchio, A.; Caillé, F.; Chevalier, A.; Loreau, O.; Horkka, K.; Halldin, C.; Schou, M.; Camus, N.; Kessler, P.; Kuhnast, B.; Taran, F.; Audisio, D. Late-Stage Isotopic Carbon Labeling of Pharmaceutically Relevant Cyclic Ureas Directly from CO_2. *Angew. Chem., Int. Ed.* **2018**, 57, 9744–9748.
(17) To circumvent this limitation the reaction time had to be significantly shorten (Scheme 6, **[^{11}C]10b**).
(18) Siodłak, D. α,β-Dehydroamino acids in naturally occurring peptides. *Amino Acids* **2015**, *47*, 1-17.
(19) a) Wright, T. H.; Bower, B. J.; Chalker, J. M.; Bernardes, G. J. L.; Wiewiora, R.; Ng, W.-L.; Raj, R.; Faulkner, S.; Vallée, M. R. J.; Phanumartwiwath, A.; Coleman, O. D.; Thézénas, M.-L.; Khan, M.; Galan, S. R. G.; Lercher, L.; Schombs, M. W.; Gerstberger, S.; Palm-Espling, M. E.; Baldwin, A. J.; Kessler, B. M.; Claridge, T. D. W.; Mohammed, S.; Davis, B. G. Posttranslational mutagenesis: A chemical strategy for exploring protein side-chain diversity. *Science* **2016**, *354*, 6312. b) Dadová, J.; Galan, S. R. G.; Davis, B. G. Synthesis of modified proteins via functionalization of dehydroalanine. *Curr. Opin. Chem. Biol.* **2018**, *46*, 71-81. c) Freedy, A. M.; Matos, M. J.; Boutureira, O.; Corzana, F.; Guerreiro, A.; Akkapeddi, P.; Somovilla, V. J.; Rodrigues, T.; Nicholls, K.; Xie, B.; Jiménez-Osés, G.; Brindle, K. M.; Neves, A. A.; Bernardes, G. J. L. Chemoselective Installation of Amine Bonds on Proteins through Aza-Michael Ligation. *J. Am. Chem. Soc.* **2017**, *139*, 18365-18375. d) Bogart, J. W., Bowers, A. A. Dehydroamino acids: chemical multi-tools for late-stage diversification. *Org. Biomol. Chem.* **2019**, *17*, 3653-3669.

(20) a) Röhm, K. H., van Etten, R. L. Stereospecific synthesis of L-[1,4-$^{13}C_2$]aspartic acid, L-β-([^{13}C]cyano)alanine and L-[4-^{13}C]aspartic acid. *J. Labelled Compd. Radiopharm.* **1985**, *22*, 909–915. b) Lodwig, S. N.; Unkefer, C. J. Stereoselective Synthesis of Stable Isotope Labeled L-α-Amino Acids: Synthesis of L−[4−^{13}C] and L−[3,4−$^{13}C_2$]Aspartic Acid. *J. Labelled Compd. Radiopharm.* **1992**, *31*, 95–102. c) Bsharat, O.; Doyle, M. G. J.; Munch, M.; Mair, B. A.; Cooze, C. J. C.; Derdau, V.; Bauer, A.; Kong, D.; Rotstein, B. H.; Lundgren, R. J. Aldehyde-catalysed carboxylate exchange in α-amino acids with isotopically labelled CO_2. *Nat. Chem.* **2022**, *14*, 1367–1374.

(21) Hutchby, M.; Houlden, C. E.; Haddow, M. F.; Tyler, S. N. G.; Lloyd-Jones, G. C.; Booker-Milburn, K. I. Switching Pathways: Room-Temperature Neutral Solvolysis and Substitution of Amides. *Angew. Chem., Int. Ed.* **2012**, *51*, 548-551.

(22) a) Benedetti Vega, K.; Campos Delgado, J. A.; Pugnal, L. V. B. L.; König, B.; Menezes Correia, J. T.; Weber Paixão, M., Divergent Functionalization of Styrenes via Radical/Polar Crossover with CO_2 and Sodium Sulfinates. *Chem. Eur. J.* **2023**, e202203625. b) Pitzer, L.; Schwarz, J. L.; Glorius, F., Reductive radical-polar crossover: traditional electrophiles in modern radical reactions. *Chem. Sci.* **2019,** *10*, 8285-8291. c) Studer, A.; Curran, D. P., Catalysis of Radical Reactions: A Radical Chemistry Perspective. Angew. Chem. Int. Ed. *2016*, 55, 58-102.

(23) Galley, G.; Godel, T.; Goergler, A.; Hoffmann, T.; Kolczewski, S.; Roever, S. 1,3,8-Triazaspiro[4.5]decan-4-one derivatives as neurokinin receptor antagonists. WO0194346A1, December 13, 2001.

(24) a) Mallikaarjun, S.; Salazar, D. E.; Bramer, S. L. *J. Clin. Pharmacol.* **2004**, *44*, 179–187. b) Abram, M.; Rapacz, A.; Mogilski, S.; Latacz, G.; Lubelska, A.; Kamiński, R. M., Kamiński, K. Multitargeted Compounds Derived from (2,5-Dioxopyrrolidin-1-yl)(phenyl)-Acetamides as Candidates for Effective Anticonvulsant and Antinociceptive Agents. *ACS Chem. Neurosci*. **2020**, *11*, 1996–2008.

(25) It is noteworthy that the animal and human metabolism and pharmacokinetics of [^{14}C]oxaprozin were reported, and shows that the carboxylic acid is metabolically stable. See: a) Janssen, F. W.; Jusko, W. J.; Chiang, S. T.; Kirkman, S. K.; Southgate, P. J.; Coleman, A. J.; Ruelius, H. W. Metabolism and kinetics of oxaprozin in normal subjects. *Clin. Pharmacol. Ther.* **1980**, *27*, 352-362. b) Janssen, F. W.; Kirkman, S. K.; Knowles, J. A.; Ruelius, H. W. Disposition of 4,5-diphenyl-2-oxazolepropionic acid (oxaprozin) in beagle dogs and rhesus monkeys. *Drug Metab. Dispos.* **1978**, *6*, 465-475.

(26) Rainsford, K. D.; Omar, H.; Ashraf, A.; Hewson, A. T.; Bunning, R. A. D.; Rishiraj, R.; Shepherd, P.; Seabrook, R. W. Recent pharmacodynamic and pharmacokinetic findings on oxaprozin. *InflammoPharmacology* **2002**, *10*, 185–239.

(27) a) Susán, A. B.; Duncan, W. P. Synthesis of 1,5,9-cyclododecatriene-x-$^{14}C_6$. *J. Labelled Compd. Radiopharm.* **1981**, *18*, 1227-1234. b) Diel, B. N.; Han, M.; White, J. M. Synthesis of [$^{14}C_6$-3,4,7,8,11,12]-(1E,5E,9E)-cyclododeca-1,5,9-triene. *J. Labelled Compd. Radiopharm.* **2007**, *50*, 407-409. c) Saunders, D.; Warrington, B. H. Syntheses of ^{14}C-labelled prizidilol dihydrochloride. *J. Labelled Compd. Radiopharm.* **1985**, *22*, 869-881.

(28) With 1.5 equivalents of [^{13}C]CO_2, **[^{13}C]7d** could be isolated enriched at 12% with 56% of yield.

(29) a) Schluter, D. N.; Mamantov, G.; Vercellotti, J. R. Electroreduction and related studies on 2-aminoacrylic acid derivatives. Part I. Electroreactivity of 2-acetamidocinnamic acid. *Journal of the Chemical Society, Perkin Transactions 2* **1973**, 1663. b) Ferreira, P. M. T.; Monteiro, L. S.; Pereira, G. Synthesis and electrochemical behaviour of β-halodehydroamino acid derivatives. *Amino Acids* **2010**, *39*, 499-513.

(30) Hendy, C. M.; Smith, G. C.; Xu, Z.; Lian, T.; Jui, N. T. Radical Chain Reduction via Carbon Dioxide Radical Anion (CO2 •−). *J. Am. Chem. Soc.* **2021**, *143*, 8987–8992. Herein, the authors showed that the olefin potential and the reaction outcome in presence of $CO_2^{\bullet-}$ are correlated. More electron-poor olefins ($E^0 \geq -2.1$ V vs SCE) undergo SET, while hydrocarboxylation prevails on less electron-poor olefins ($E^0 \leq -2.1$ V vs SCE).

(31) Parnes, H. A method for the preparation of ^{14}C-labeled carboxylic acids. Synthesis of 6,11-dihydro[b,e]thiepin-11-one-3-yl acetic ^{14}C-acid. *J. Labelled Compd. Radiopharm.* **1979**, *16*, 771–775.
(32) This representative family of molecules have been labeled in tedious, multi-step manners. a) Blackburn, C. E. Carbon-14 and tritium labelling of *m*-(1-methyl-3-propyl-pyrrolidinyl)- phenol monohydrochloride (profadol; CI-572) *J. Labelled Compd.* **1970**, *6*, 21-33. b) Somayaji, V. V.; Hall, T. W.; Wiebe, L. I.; Knaus, E. E.; Demers, J. P. Synthesis of [5-^{14}C]-1,1,12,12-tetraethoxy-4,9-diazadodecane dinitrate. *J. Labelled Compd. Radiopharm.* **1989**, *27*, 449-455. c) Nishioka, K.; Kanamaru, H. ^{14}C-labeling of a novel anxiolytic agent tandospirone. *J. Labelled Compd. Radiopharm.* **1992**, *31*, 427-436.
(33) Enquist, J.; Krishnan, S.; Atwal, S.; Erlanson, D.; Fucini, R. V.; Hansen, S.; Sawayama, A.; Sethofer, S. Modulators of G-Protein Coupled Receptors. U.S Patent WO2019183577A1, September 26, 2019.
(34) Verschueren, W. G.; Dierynck, I.; Amssoms, K. I. E.; Hu, L.; Boonants, P. M. J. G.; Pille, G. M. E.; Daeyaert, F. F. D.; Hertogs, K.; Surleraux, D. L. N. G.; Wigerinck, P. B. T. P. Design and Optimization of Tricyclic Phtalimide Analogues as Novel Inhibitors of HIV-1 Integrase. *J. Med. Chem.* **2005**, *48*, 1930–1940.
(35) Wu, L. I. Gemcitabine Prodrugs and Uses Thereof. US2014134160A1, May 15, 2014.
[36] a) Simmons, E. M.; Hartwig, J. F., On the Interpretation of Deuterium Kinetic Isotope Effects in C-H Bond Functionalizations by Transition-Metal Complexes. *Angew. Chem. Int. Ed.* **2012,** *51*, 3066-3072. b) Wang, L.; Xia, Y.; Derdau, V.; Studer, A., Remote Site-Selective Radical C(sp3)−H Monodeuteration of Amides using D_2O. *Angew. Chem. Int. Ed.* **2021,** *60*, 18645-18650.
(37) Forgács, V.; Németh, E.; Gyuricza, B.; Kis, A.; Szabó, J. P.; Mikecz, P.; Mátyus, P.; Helyes, Z.; Horváth, Á. I.;Kálai, T.; Trencsényi, G.; Fekete, A.; Szikra, D. Radiosynthesis and Preclinical Investigation of ^{11}C-Labelled 3-(4,5-Diphenyl-1,3-oxazol-2-yl)propanal Oxime ([^{11}C]SZV 1287). *ChemMedChem* **2020**, *15*, 2470–2476.